5-Substituted Tetrazoles as Bioisosteres of Carboxylic Acids. Bioisosterism and Mechanistic Studies on Glutathione Reductase Inhibitors as Antimalarials

Christophe Biot,*,† Holger Bauer,‡,§,|| R. Heiner Schirmer,|| and Elisabeth Davioud-Charvet*,‡,§,||

Bioinformatique Génomique et Structurale, CP 165/61, Université Libre de Bruxelles, 50 Av. F. D. Roosevelt, B-1050 Brussels, Belgium, UMR 8525 CNRS-Université Lille II-Institut Pasteur de Lille, Institut de Biologie de Lille, 1 rue du Professor Calmette, BP447 59021 Lille Cedex, France, and Biochemie-Zentrum der Universität Heidelberg, Im Neuenheimer Feld 504, 69120 Heidelberg, Germany

Received March 30, 2004

Plasmodium parasites are exposed to elevated fluxes of reactive oxygen species during intraerythrocytic life. The most important antioxidative systems are based on the glutathione reductases of the malarial parasite *Plasmodium falciparum* and the host erythrocyte. The development of menadione chemistry has led to the selection of the carboxylic acid 6-[2′-(3′-methyl)-1′,4′-naphthoquinolyl] hexanoic acid **M$_5$** as an inhibitor of the parasitic enzyme. As reported here, revisiting the mechanism of **M$_5$** action revealed an uncompetitive inhibition type with respect to both NADPH and glutathione disulfide. Masking the polarity of the acidic function of **M$_5$** by ester or amide bonds improved antiplasmodial activity. Bioisosteric replacement of the carboxylic function by tetrazole to increase bioavailability and to maintain comparable acidity led to improved antimalarial properties as well, but only with the cyanoethyl-protected tetrazoles. Using computed ab initio quantum methods, detailed analyses of the electronic profiles and the molecular properties evidenced the similarity of **M$_5$** and the bioisoteric tetrazole **T$_4$**. The potential binding site of these molecules is discussed in light of the recently solved crystallographic structure of *P. falciparum* enzyme.

Introduction

The prevalence of malaria in many parts of the world, together with the lack of vaccines and the emergence of highly resistant strains of *Plasmodium falciparum* to widely used antimalarial drugs such as chloroquine, make it necessary to search for new antiplasmodial molecules. For the following reasons we have focused on inhibitors of glutathione reductase (GR) as antimalarial agents.[1,2] GR catalyzes the reaction (eq 1) where GSSG is glutathione disulfide and GSH reduced glutathione.

$$\mathrm{GSSG} + \mathrm{NADPH} + \mathrm{H^+} \rightarrow 2\,\mathrm{GSH} + \mathrm{NADP^+} \quad (1)$$

Ginsburg et al. had observed that the chloroquine concentration needed to kill parasites is inversely related to GSH levels.[3] Moreover, Müller et al. confirmed the previous observation by demonstrating a clear correlation between the levels of glutathione and the degree of chloroquine resistance in different *P. falciparum* strains.[4] Recently potentiation of the antimalarial action of chloroquine was demonstrated in rodent malaria by drugs known to reduce cellular glutathione levels.[5] This emphasized the importance of GSH in the development of chloroquine resistance. The maintenance of intracellular glutathione in *P. falciparum* is mainly dependent on glutathione synthesis, GSSG efflux, and GSSG reduction catalyzed by GR or promoted by reduced thioredoxin. The 2.6 Å resolution crystal structure of *P. falciparum* GR has recently been determined.[6] The amino acid sequences of the parasitic and the human enzyme share 40% identity. Notably, there are pronounced differences between the human and the parasite enzymes in the shape and electrostatics of a large cavity at the dimer interface. This cavity binds numerous noncompetitive or uncompetitive inhibitors and is a target for selective drug design. It is lined by 22 amino acid residues in *P. falciparum* GR and by 24 residues in human GR. Also, the charges of the cavity walls are very different, with the *P. falciparum* GR cavity being rather neutral while the human GR cavity is negatively charged. Moreover, the two residues Phe78 and Phe78′, which stabilize the 2-methyl-1,4-naphthoquinone (menadione, Chart 1) through aromatic $\pi-\pi$ stacking interactions in human GR·menadione crystal complexes,[7] are absent in *P. falciparum* GR cavity. This suggests a different mode of binding for potential inhibitors of *P. falciparum* GR versus human GR.

Previously, we have demonstrated that the naphthoquinone carboxylic acid **M$_5$** (Chart 1) is a potent *P. falciparum* GR inhibitor.[8] We now postulate that the weak in vitro antimalarial activity observed with **M$_5$** ($IC_{50} = 3.5\ \mu M$ against the chloroquine-resistant strain FcB1R) depends on a weak cellular penetration due to the presence of the carboxylic acid function which is necessary for GR binding. In order to mask the polarity of the carboxylate group, our work was aimed at a prodrug approach to increase the overall lipophilicity of the molecule and to promote membrane permeability.

* To whom correspondence should be addressed. E.D.-C.: tel, +49-6221-54-4188; fax, +49-6221-54-5586; e-mail, elisabeth.davioud@gmx.de. C.B.: tel, (33) 03 20 43 48 93; fax, (33) 03 20 43 65 85; e-mail, christophe.biot@ensc-lille.fr.

† Université Libre de Bruxelles.

‡ Institut de Biologie de Lille.

§ Delegate (E.D.-C.) and Fellow (H.B.) of Centre National de la Recherche Scientifique, France in the frame of a French−German cooperation with the University of Heidelberg, Germany.

|| Biochemie-Zentrum der Universität Heidelberg.

10.1021/jm0497545 CCC: $27.50
Published on Web 10/26/2004

Chart 1

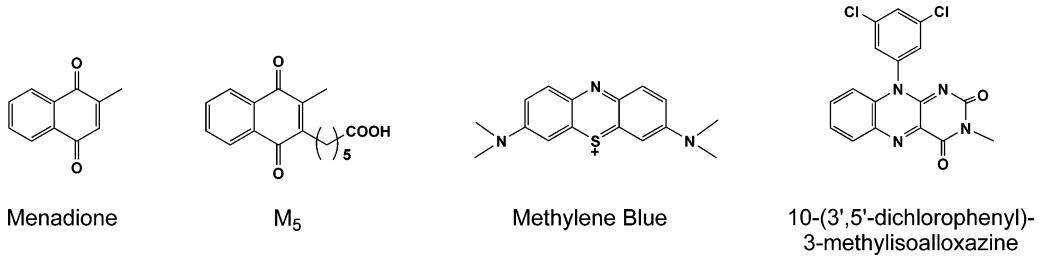

Scheme 1. Synthesis of Aminoester Prodrugs Based on the $\mathbf{M_5}$ Structure[a]

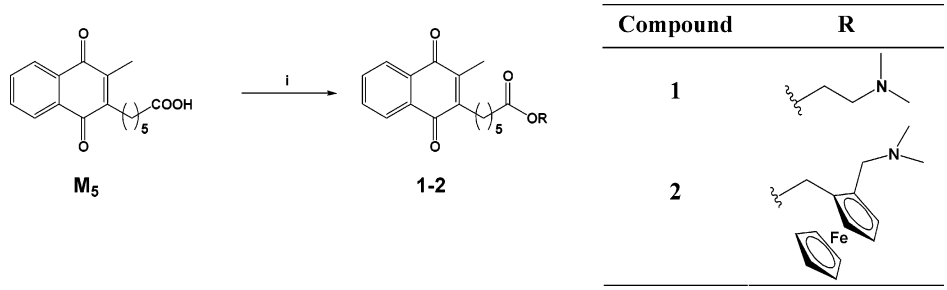

[a] Reagents and conditions: (i) ROH, DCC, DMAP, CH_2Cl_2, 0 °C for 1 h, then room temperature for 12 h.

First, we prepared two esters containing a basic amino group that is suggested to play an important role in drug accumulation through pH-dependent trapping (via protonation). A lipophilic ferrocenyl moiety which can provide better bioavailability mostly by facilitating the membrane passage was also introduced. As isosteric replacement of the carboxylic acid with tetrazole often preserves or improves the biological activities of the parent drug, a series of bioisosteric tetrazoles based on the $\mathbf{M_5}$ structure was designed and synthesized in order to increase the cell penetration. Indeed, the tetrazole moiety is comparable in size and in acidity to the −COOH group and, moreover, it is metabolically more stable.[9] The related analogues based on $\mathbf{M_3}$ and $\mathbf{M_4}$ were also synthesized to evaluate the influence of the spacer length between the naphthoquinone and the tetrazole. Indeed, as reported in our earlier paper, the most potent GR inhibitor $\mathbf{M_5}$ competed with GSSG at low concentrations but not any more at high GSSG concentrations; this latter observation was not detailed further.[8] Kinetics studies were performed with $\mathbf{M_5}$ in order to determine the inhibition type under cell-pathological conditions, i.e., at 1 mM GSSG. In parallel, intrinsic molecular properties of the ligands such as size and volume, molecular electrostatic potentials, and charge distribution were computed by ab initio quantum methods to complete the structure−activity relationships in view of the recently resolved crystal structure of the *P. falciparum* GR (PDB code: 1ONF). The studied electronic profiles were also discussed.

Results

Chemistry. The esters **1** and **2** were obtained from reacting $\mathbf{M_5}$ with *N*,*N*-dimethylethanolamine and 2-(*N*,*N*-dimethylaminomethyl)ferrocenyl-methanol, respectively, by esterification in the presence of dicyclohexylcarbodiimide (DCC) and *N*,*N*-dimethylaminopyridine (DMAP) in dried CH_2Cl_2 (Scheme 1). For the preparation of the bioisosteric tetrazole analogues of $\mathbf{M_3}$−$\mathbf{M_5}$, we first attempted the 1,3-cycloaddition of the nitrile analogue of $\mathbf{M_5}$ with an inorganic azide (NaN_3) using an amine salt ($Et_3N{\cdot}HCl$) in toluene (reflux, 15 h).[10] However, this reaction did not lead to the desired tetrazole $\mathbf{T_5}$. Under these conditions, addition of the azide to the carbonyl groups of the naphthoquinone is faster than to the nitrile of the side chain and the diazido derivative was obtained (data not shown). As an alternative route, we applied the elegant introduction of the protected tetrazole described by De Lombaert et al.,[11] but with modified conditions (Scheme 2). We examined the reaction between the carboxamides **3**−**5**—obtained from $\mathbf{M_3}$−$\mathbf{M_5}$ and amino-2-propionitrile—and NaN_3 under mild conditions (room temperature) in order to avoid the addition of the azide to the keto group. For completion of the reaction, 4 equiv of triflic anhydride was required instead of 1 equiv in the reported method.[11] A probable explanation is that there is a reversible addition of CF_3-SO_2 to the keto groups of the quinone moiety, which are then regenerated during the workup by hydrolysis. The purified protected tetrazoles **6**−**8** were obtained almost quantitatively. Subsequently, various bases were examined for the β-H elimination of the 2-cyanoethyl group: LiOH proved to be the most efficient treatment to yield the pure tetrazoles $\mathbf{T_3}$−$\mathbf{T_5}$. Organic bases (such as DBU or TBAF) produced compounds of lower purity which were more difficult to separate. As an example, the tetrazole $\mathbf{T_4}$ is prepared from $\mathbf{M_4}$ with 55% yield through the three-step procedure described in Scheme 2 (**4**, 81% yield; **7**, 75% yield; $\mathbf{T_4}$, 90% yield).

Antimalarial Activity. The antiplasmodial activity of the new compounds was evaluated in assays using the moderately chloroquine resistant strain FcB1R of *P. falciparum*. In parallel, their toxicity was evaluated against the human diploid embryonic lung cell line hMRC-5 (Table 1). Specifically, we tested prodrugs and bioisosteres of the antimalarial carboxylic acids $\mathbf{M_3}$−$\mathbf{M_5}$ that were previously reported as potent inhibitors of glutathione reductase from *P. falciparum*.[8,12] Most of the newly described compounds **1**−**8** displayed increased antiplasmodial activities (IC_{50} values around 1 μM for **2**−**8**) when compared with the parent carboxylic acids $\mathbf{M_3}$−$\mathbf{M_5}$ (IC_{50} values ranging from 2 to 4 μM). In

Scheme 2. Synthesis of Tetrazoles $\mathbf{T_3}$−$\mathbf{T_5}$[a]

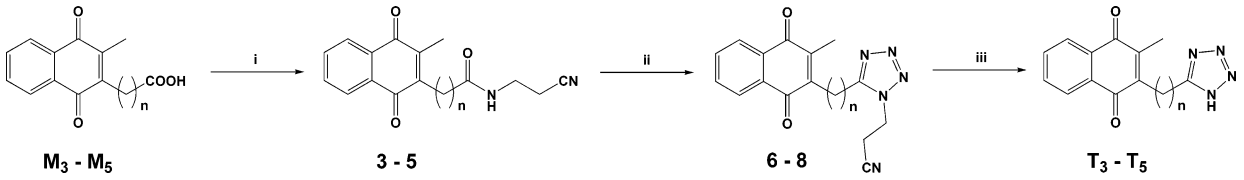

[a] Reagents and conditions: (i) 1.3 equiv of $NC(CH_2)_2NH_2$, 1 equiv of HOBt, 1.2 equiv of EDC, DMF, 0 °C for 1 h, then room temperature for 5 h; (ii) 1.1 equiv of NaN_3, 4 equiv of $(CF_3SO_2)_2O$, CH_3CN, room temperature, 20 h; (iii) 1.2 equiv of $LiOH{\cdot}H_2O$, THF, MeOH, room temperature, 2 h.

Table 1. In Vitro Sensitivity of the *P. falciparum* FcB1R Strain[a] toward the Prodrug Esters **1** and **2**, the Carboxamides **3**−**5**, and the Tetrazoles **6**−**8**[b,c]

Compound	IC_{50} for FcB1R[a,d] (μM)
Ester and Amide Prodrugs Based on the GR Inhibitor M_5	
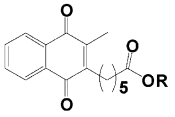	
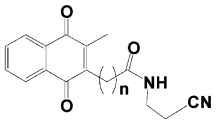	
1	12.6 ± 1.9
2	1.0 ± 0.1
1 R = 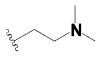 **3** n = 3	**3** 1.8 ± 0.1[c]
4 n = 4	**4** 1.5 ± 0.4[c]
2 R = 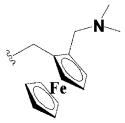 **5** n = 5	**5** 1.0 ± 0.1[c]
Tetrazole Prodrugs Based on M_3-M_5 Analogs	
	M_3 2.2[b]
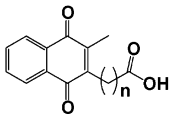 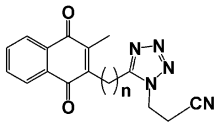	**M_4** 4.0[b]
	M_5 3.5[b]
M_3 n = 3 **6** n = 3	**6** 0.9 ± 0.0[c]
M_4 n = 4 **7** n = 4	**7** 1.4 ± 0.2[c]
M_5 n = 5 **8** n = 5	**8** 1.1 ± 0.1[c]

[a] As controls, IC_{50} values of 126 ± 28 nM and 3.5 ± 0.3 μM were determined for chloroquine and the starting alcohol of ester **2**, 2-(*N,N*-dimethylaminomethyl)ferrocenyl-methanol. [b] Values from ref 8. [c] Values from ref 12. [d] The compounds were also tested for cytotoxic effects on hMRC-5 cells. The compounds listed here showed no cytotoxicity against the human diploid embryonic lung cell line hMRC-5 (Bio-Whittaker 72211D), when tested at concentrations of up to 32 μM.

addition, none of them displayed cytotoxicity at concentrations of up to 32 μM against the human cell line hMRC-5 (Table 1). Aminoester **1** is a weak base that was expected to penetrate through the membranes of parasitized erythrocytes and to be sequestered in acidic compartments by proton trapping, as observed with many other basic drugs. Obviously, ester **1** was found to behave very differently from weak bases previously reported with respect to cell uptake.[8] In addition, the activity of aminoester **1** is much lower than that of the parent carboxylic acid $\mathbf{M_5}$, in contrast to the expected prodrug effect. This observation suggests that the subcellular distribution of aminoester **1** does not follow that of parent carboxylic acids due to different partition coefficients, especially in infected erythrocytes.

The rationale for aminoester **2** was based on the introduction of highly lipophilic moieties in addition to dialkylamino groups. In a previous study (unpublished data), we had found that the metallocenic alcohol, 2-(*N,N*-dimethylaminomethyl)ferrocenyl-methanol, showed a significant antimalarial activity per se (Table 1, footnote *a*) in the same range as their carboxylic acid counterparts $\mathbf{M_3}$−$\mathbf{M_5}$. As for $\mathbf{M_5}$, it seems that starting ferrocenyl alcohol could be either specifically taken up by infected red blood cells or recognized by specific targets in the parasite since no cytotoxicity was revealed at concentrations of up to 32 μM against the human cell line hMRC-5. The design of compound **2** was based on the combination of both bioactive moieties linked by an ester bond. Out of the two esters, only ester **2** exhibited a greater antimalarial activity than both parent molecules. This increased activity is probably mediated by a double-drug effect leading to the release of the two active components in the parasite.

Permeation enhancement of $\mathbf{M_5}$ has led to the design of alkyltetrazoles as carboxylic acid bioisosteres. It is

Table 2. $\mathbf{M_5}$ Derivatives as Inhibitors of *P. falciparum* GR and Human GR

	IC_{50} (μM)	
compound	*P. falciparum* GR	human GR
$\mathbf{M_5}$	4.5[a]	3.2[a]
4	57.0	22.7
7	10.8	27.0
MB	6.4[b]	16.0[b]

[a] The inhibition parameters determined for $\mathbf{M_5}$ in previous studies for human GR[8] had a competitive component at lower substrate concentration. This was eliminated here by using a GSSG concentration of 1 mM. [b] Values from ref 40.

noteworthy that all 5-substituted tetrazoles described so far were aryltetrazoles. It is known that anionic tetrazoles are almost 10-fold more lipophilic than the corresponding carboxylates. In addition, the distribution of the charge over a greater molecular surface area may be favorable for protein−ligand recognition. However, tetrazoles do not lead always to the expected bioisosteric binding to the target, illustrating the Janus behavior of these molecules.[9] In our study, the tetrazoles $\mathbf{T_3}$−$\mathbf{T_5}$ themselves showed a poor antimalarial activity (with IC_{50} values ranging from 15 to 30 μM), which is probably due to the observed high instability of the molecules in solution.[12] This propensity to degradation might also explain the relatively poor effects of the molecules when assayed as inhibitors of glutathione reductases; they were even less active than their parent carboxylic acids $\mathbf{M_3}$−$\mathbf{M_5}$. Surprisingly, the three carboxamides **3**−**5** and the three cyanoethyl-protected tetrazoles **6**−**8** showed the highest antimalarial activities within the series. Despite the presence of the poorly cleavable amide bond (by comparison with ester bond) and the base-sensitive cyanoethyl protection of the tetrazoles, it is tempting to speculate that these compounds behave as prodrugs of the carboxylic acids $\mathbf{M_3}$−$\mathbf{M_5}$ and the tetrazoles $\mathbf{T_3}$−$\mathbf{T_5}$, respectively. However, the simultaneous inhibition of glutathione reductase and, possibly, other targets, including proteases, may result in potentiation of the antimalarial activity by interfering with the redox equilibrium and parasite development.

Glutathione Reductase Inhibition Studies. All chemical intermediates and products were studied as inhibitors of the GRs from *P. falciparum* and humans. Since the tetrazoles $\mathbf{T_3}$−$\mathbf{T_5}$ are highly instable in solutions, they were not included in the kinetic studies. Aminoesters **1** and **2** were not active in standard GR assays. The IC_{50} values of the protected tetrazoles **6** (n = 3) and **7** (n = 4) were compared in standard assays using 200 μM GSSG. While the protected tetrazole **7** showed a higher specificity than **6** with respect to the parasitic enzyme (IC_{50} values: 6 μM for **7** versus 30 μM for **6**), no difference was observed with respect to the human enzyme (IC_{50} values: 20 μM for **6** and for **7**). Furthermore, a detailed investigation of the series defined by four methylene groups was performed in comparison with $\mathbf{M_5}$ and methylene blue (MB) as references for GR inhibition at 1 mM GSSG concentration (Table 2). Under these cell-pathological conditions where the GSSG level starts to be toxic for the parasite, only very few inhibitors described earlier in the literature are still found to be potent inhibitors in both GR assays: methylene blue, some arylisoalloxazines (Chart 1), and $\mathbf{M_5}$ displayed IC_{50} values $\leq$10 μM. Among these, $\mathbf{M_5}$ is the most potent inhibitor of both *P. falciparum* GR and human GR, displaying IC_{50} values of 4.5 μM and 3.2 μM, respectively. As expected for human GR assays, the carboxamide **4** (IC_{50} = 22.7 μM) and the cyanoethyl-protected tetrazole **7** (IC_{50} = 27.0 μM) showed low inhibitory potencies when compared to $\mathbf{M_5}$ because the polarity and the charge of the functional groups are masked. However, in the *P. falciparum* GR assays, while the carboxamide **4** (IC_{50} = 57.0 μM) is a poor inhibitor, the cyanoethyl-protected tetrazole **7** (IC_{50} = 10.8 μM) acts as a significant inhibitor, suggesting that different structural requirements are essential to inhibit the parasitic enzyme. Another explanation could be also based on a catalyzed base-dependent β-H elimination of acrylonitrile to liberate the tetrazole moiety $\mathbf{T_4}$ close to the active site of *P. falciparum* GR.

Revisiting Inhibition Type of *P. falciparum* GR by $\mathbf{M_5}$. In order to investigate the outcome of GR inhibition at varying GSSG concentrations, kinetic studies were first performed using saturating substrate concentrations in the presence of $\mathbf{M_5}$. The data were fitted to the appropriate equation with Kaleidagraph using a computerized least-squares regression program. With NADPH (8−100 μM) as variable substrate and GSSG at a constant concentration of 1 mM, the K_m value for NADPH in the absence of inhibitor was 12.5 ± 1.5 μM. Assuming uncompetitive inhibition, the K_i value for $\mathbf{M_5}$ was determined as 3.7 ± 0.36 μM with respect to NADPH. With GSSG (18−900 μM) as variable substrate and NADPH at a constant concentration of 100 μM, the K_m value for GSSG in the absence of inhibitor was found to be 114.7 ± 3.6 μM. The inhibition of *P. falciparum* GR by $\mathbf{M_5}$ (0−10 μM) was also uncompetitive with respect to GSSG. The K_i value for $\mathbf{M_5}$ was determined as 3.6 ± 0.23 μM. The uncompetitive type of inhibition of *P. falciparum* GR by $\mathbf{M_5}$ was derived from Lineweaver-Burk, Dixon, and Cornish-Bowden plots (Figure 1a−d).[13] In order to prove the essential requirement of NADPH or $NADP^+$ for $\mathbf{M_5}$ binding to the binary complexes, kinetics studies were performed in the presence of glucose-6-phosphate dehydrogenase (G6PDH) and glucose-6-phosphate to recycle $NADP^+$ to NADPH. Under these conditions, this results in a high ratio of [NADPH]/[$NADP^+$]. The IC_{50} values of $\mathbf{M_5}$ (1.8 μM and 2.7 μM with human and *P. falciparum* GRs, respectively) were 2-fold lower than the values determined in the absence of the G6PDH system under the same conditions. In another experiment, we measured the IC_{50} value of $\mathbf{M_5}$ in the presence of exogenous $NADP^+$. In the presence of 200 μM $NADP^+$, the IC_{50} value of $\mathbf{M_5}$ (2.5 μM with *P. falciparum* GR) was again 2-fold lower when compared to the value determined in the absence of exogenous $NADP^+$. These results suggest that $\mathbf{M_5}$ can bind to both the binary E·NADPH and E·$NADP^+$ complexes of the GR enzyme (E) and, consequently, that the binding of $\mathbf{M_5}$ is promoted by prior association of *P. falciparum* GR with NADPH or $NADP^+$.

***P. falciparum* GR Catalyzed Naphthoquinone Reductase Activity.** The ability of *P. falciparum* GR to reduce the naphthoquinone moiety was studied by following the oxidation of NADPH in the presence of $\mathbf{M_5}$. The naphthoquinone reductase activity of *P. falciparum* GR was compared to the intrinsic NADPH oxidation activity of the enzyme in the absence of

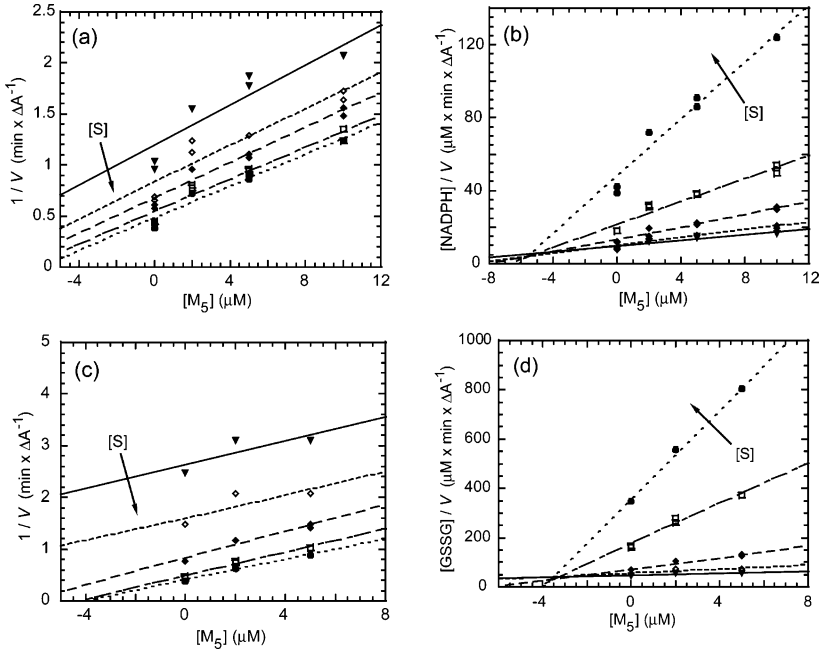

Figure 1. Inhibition of *P. falciparum* glutathione reductase by 6-[2′-(3′-methyl)naphthoquinolyl]hexanoic Acid (**M$_5$**). The assays were performed using variable concentrations of one substrate and saturation concentration of the second substrate. The kinetic data for inhibition of GR by **M$_5$** are presented in Dixon plots (panels a and c) and Cornish-Bowden plots (panels b and d). They represent two independent experiments; each experimental point was measured in duplicate. Panel a and panel b: Dixon plot and Cornish-Bowden plot, respectively, for **M$_5$** and NADPH in the presence of 1 mM GSSG. [NADPH]: 100 μM (●), 40 μM (□), 20 μM (◆), 12 μM (◇), 8 μM (▼). [**M$_5$**]: 0, 2, 5, and 10 μM. Panel c and panel d: Dixon plot and Cornish-Bowden plot, respectively, for **M$_5$** and GSSG in the presence of 100 μM NADPH. [GSSG]: 900 μM (●), 360 μM (□), 90 μM (◆), 36 μM (◇), 18 μM (▼). [**M$_5$**]: 0, 2, and 5 μM.

naphthoquinone (NQ) (eq 2). *P. falciparum* GR displayed a 7-fold higher NADPH oxidation activity in the presence of 400 μM **M$_5$** (eq 3 or 4); the observed NADPH oxidation rates were 0.012 unit/mg protein in the absence of naphthoquinone and 0.085 unit/mg protein in the presence of 400 μM **M$_5$**.

$$2O_2 + NADPH + H^+ \rightarrow 2O_2^{-\bullet} + NADP^+ + 2H^+ \quad \text{(enzymatic)} \quad (2)$$

$$2NQ + NADPH + H^+ \rightarrow 2NQ^{-\bullet} + NADP^+ + 2H^+ \quad \text{(enzymatic)} \quad (3)$$

$$NQ + NADPH + H^+ \rightarrow NQH_2 + NADP^+ \quad \text{(enzymatic)} \quad (4)$$

The K_m and k_{cat} values, 109.0 ± 10.6 μM and 0.103 ± 0.004 s^{-1}, corresponding to $V_{max} = 0.107$ unit/mg protein were derived from measurements at 10 different substrate concentrations. When following NADPH consumption, **M$_5$** was reduced by *P. falciparum* GR with a catalytic efficiency k_{cat}/K_m of 945 M^{-1} s^{-1}, a value 18-fold lower than that determined for methylene blue (data not shown). These data are also in good agreement with previous observations on menadione reported by Nordhoff[14] and Blumenstiel et al.[15] These last authors studied menadione at a concentration of 100 μM as an inhibitor and as a substrate of human GR. Reduction of 1 mM GSSG was inhibited by 75%, and the turnover for menadione as a substrate was determined to be 0.043 unit/mg. We repeated these experiments[14,15] and confirmed that menadione behaved as an uncompetitive inhibitor of human GR with respect both to NADPH and to glutathione disulfide, the K_i values of menadione being 16.1 ± 2.2 μM and 12.1 ± 2.6 μM, respectively. When menadione was studied as a substrate of human and *P. falciparum* GRs, the k_{cat} values were determined as 0.16 ± 0.02 s^{-1} for both enzymes and the K_m values as 31.2 ± 1.4 μM and 82.2 ± 22.2 μM, respectively. This results in a catalytic competence k_{cat}/K_m of 5330 M^{-1} s^{-1} for the human enzyme and of 1991 M^{-1} s^{-1} for the parasitic enzyme. Since the product was unable to reduce cytochrome *c* (eq 5), which requires a one-electron transfer, it was concluded[14] that the product of menadione reduction was menadiol (eq 4).

$$NQ^{-\bullet} \text{ (or } O_2^{-\bullet}) + \text{cyt } c\ (Fe^{3+}) \rightarrow NQ \text{ (or } O_2) + \text{cyt } c\ (Fe^{2+}) \quad \text{(non enzymatic)} \quad (5)$$

Modeling Studies. As discussed above for human GR and *P. falciparum* GR, certain uncompetitive and noncompetitive inhibitors bind in a cavity distinct from the binding sites for GSSG and NADPH.[16−21] In human GR, this cavity was shown to be the binding site of menadione,[17] 3,7-diamino-2,8-dimethyl-5-phenylphenazinium chloride (safranin),[17] 6-hydroxy-3-oxo-3*H*-xanthene-9-propionic acid,[18] a series of 10-arylisoalloxazines,[19] *S*-(2,4-dinitrophenyl)glutathione,[20] and methylene blue.[6,21] To identify the factors discriminating between the cavities of human and parasite enzymes, a detailed analysis of the electronic profiles of **M$_5$** and its tetrazole analogues was performed.

Optimized Geometry of the Carboxylic Acids and Tetrazoles. In the absence of X-ray data, the HF/6-31G** optimized geometries for **M$_3$**−**M$_5$** and **T$_3$**−**T$_5$** were generated in a vacuum (Table 3a). A comparison of the minimal energy conformers of **T$_3$**−**T$_5$** with **M$_5$**

Table 3. Structural and Electronic Profiles of the Carboxylate $\mathbf{M_5}$ and the Tetrazolate $\mathbf{T_4}$[a]

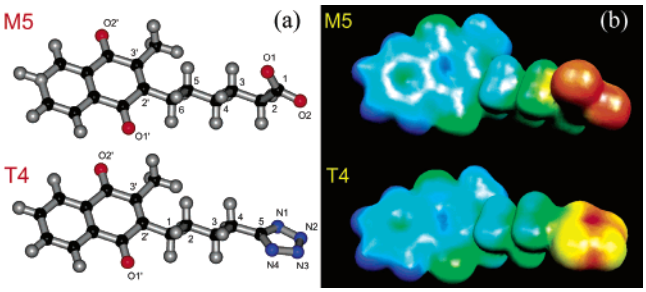

(c) Atomic Electrostatic Charge Densities of $\mathbf{M_5}$ and $\mathbf{T_4}$ Anions

$\mathbf{M_5}$		$\mathbf{T_4}$	
atom	anion charge density	anion charge density	atom
C1′	+0.56	+0.56	C1′
C2′	−0.09	−0.09	C2′
C3′	−0.11	−0.11	C3′
C4′	+0.56	+0.56	C4′
C5′	−0.08	−0.08	C5′
C6′	+0.01	+0.01	C6′
C7′	+0.01	+0.01	C7′
C8′	+0.09	+0.09	C8′
C9′	−0.12	−0.12	C9′
C10′	−0.12	−0.12	C10′
O1′	−0.55	−0.56	O1′
O2′	−0.54	−0.54	O2′
C1	+0.74	+0.42	C5
C2	−0.15	−0.02	C4
C3	+0.03	+0.03	C3
C4	−0.03	+0.00	C2
C5	+0.02	+0.06	C1
C6	+0.05		
O1	−0.76	−0.50	N1
O2	−0.77	−0.18	N2
		−0.19	N3
		−0.49	N4

[a] (a) Representation of the optimized geometries of the deprotonated forms $\mathbf{M_5}$ and $\mathbf{T_4}$. Carbon atoms are colored in black, hydrogen atoms in gray, oxygen atoms in red, and nitrogen atoms in blue. The images were generated using Insight II (Accelrys Inc.). (b) Molecular electrostatic potential energy isosurfaces of the deprotonated forms of $\mathbf{M_5}$ and $\mathbf{T_4}$. The color code is in the range of −210 (deepest red) to +10 (deepest blue) kcal/mol. Images were generated using Molekel.[47] (c) Atomic electrostatic charge densities of $\mathbf{M_5}$ and $\mathbf{T_4}$ anions calculated at the HF/6-31G** level (with hydrogens summed into heavy atoms).

shows that the most potent GR inhibitor, the tetrazole derivative $\mathbf{T_4}$, presents the values most similar to those of $\mathbf{M_5}$ with respect to their interatomic distances. For $\mathbf{T_4}$, the C3′···C5 distance (respectively C3′···C2 distance in $\mathbf{M_5}$) is shorter with 7.12 Å versus 7.18 Å, the C2′···C5 distance (respectively C2′···C2 distance in $\mathbf{M_5}$) with 6.39 Å versus 6.43 Å, and the CH_3···C5 distance (respectively CH_3···C2 distance in $\mathbf{M_5}$) with 6.96 Å versus 7.04 Å. For $\mathbf{M_5}$, the C2′−C3′−C2 angle is 119.18°, and for $\mathbf{T_4}$ the corresponding C2′−C3′−C5 angle is 118.10°. For $\mathbf{M_5}$ the C3′−C2′−C2 angle is 51.45° whereas for $\mathbf{T_4}$ the corresponding C3′−C2′−C5 angle is 52.35°. Finally, atomic superposition of compounds $\mathbf{T_4}$ and $\mathbf{M_5}$ shows a high overlap with a root-mean-square value close to zero (Table 3a). As a cautionary note, these inhibitors may adopt different conformations, due to the high flexibility of the alkyl chain, when binding to the active site of *P. falciparum* GR. The molecular volume (MV) of the six inhibitors has also been calculated and compared to that of methylene blue. MV is defined as the volume inside a contour of 0.001 electron/bohr^3 density and can be computed to an accuracy of about 10%. $\mathbf{M_5}$ (MV = 366 Å^3), $\mathbf{T_4}$ (MV = 363 Å^3), and methylene blue (MV = 355 Å^3) possess roughly the same size and this volume which fits the cavity at the dimer interface of *P. falciparum* GR (ca. 450 Å^3).[6]

Molecular Electrostatic Potentials and Charge Distribution. As the electrostatic surface potential has been shown to be a useful parameter in describing different molecular interactions,[22] we computed this quantity for the most potent inhibitors $\mathbf{M_5}$ and $\mathbf{T_4}$ (Table 3b). The most positive potentials (colored in blue) represent the naphthoquinone moiety whereas the most negative potentials (colored in red) are located around the carboxylate and the tetrazole group for $\mathbf{M_5}$ and $\mathbf{T_4}$, respectively. Moreover, the molecular electrostatic potentials (MEP) of $\mathbf{M_5}$ and $\mathbf{T_4}$ showed remarkable similarity; noteworthy are the substantial differences in the most negative wrap of the electrostatic surface due to the delocalization of the charge on the nitrogens and the carbon of the tetrazole ring in $\mathbf{T_4}$ (Table 3c). Thus, the so contrasted MEPs, between the π-system of the naphthoquinone moiety and the anionic head, suggest a specific recognition pattern in the *P. falciparum* GR cavity involving the close proximity of a hydrophobic pocket (and/or (partially) charged residues able to give cation−π interactions) and of salt bridges. From Table 3c, it follows that charge distribution in $\mathbf{M_5}$ and $\mathbf{T_4}$ is quite similar with respect to the naphthoquinone moiety and the alkyl side chain, but differs at their polar functions, i.e., the strong electron-withdrawing carboxylate and tetrazolate anions.

HOMO and LUMO Eigenvalues. These values were calculated at the HF/6-31G** level of theory. The calculations suggest that the LUMO state of $\mathbf{M_5}$ and $\mathbf{T_4}$ is localized on the naphthoquinone core and the HOMO state is localized on the anionic group, the carboxylate and the tetrazolate moiety, respectively. It is interesting to note here that while the HOMO and LUMO energy levels were clearly similar in the case of $\mathbf{M_5}$ (ϵ_{HOMO} = −4.68 eV/ϵ_{LUMO} = +2.59 eV) and $\mathbf{T_4}$ (ϵ_{HOMO} = −4.45 eV/ϵ_{LUMO} = +2.59 eV) and different from those of methylene blue (ϵ_{HOMO} = −10.37 eV/ϵ_{LUMO} = −3.16 eV), their band gap (defined as $\epsilon_{LUMO} - \epsilon_{HOMO}$) was ca. 7 eV in all cases, suggesting very similar electronic properties for these structurally unrelated compounds. Calculations performed using a higher theory level including electron correlation contributions (MP2/6-31G**) confirmed these results (data not shown).

Discussion

Antimalarial Activity. The presence of the acidic function in the glutathione reductase inhibitor $\mathbf{M_5}$ is essential for binding to its target, but tends to be excluded from acidic, membrane-bounded compartments. In our previous efforts to enhance the antiparasitic action of glutathione reductase inhibitors, double-headed prodrugs based on 4-aminoquinoline moieties and the glutathione reductase inhibitor $\mathbf{M_5}$ were designed to direct the inhibitor to the parasitic compartment.[8] The double-drug esters revealed a potent antimalarial action, thus validating our strategy. Our present study represents a first attempt to design new $\mathbf{M_5}$-like molecules with improved pharmacokinetic profiles and drug-like properties, especially with molecular

weights below 500. Reversible masking of the carboxylate group was assumed to allow accumulation of the compound in the acidic digestive compartments. In particular, this may be true if the starting alcohol used in the esterification reaction of **M$_5$** possesses dialkylamino groups. For instance, aminoesters **1** and **2** are weak bases that were expected to penetrate infected red blood cells and accumulate by proton trapping to a larger extent than the parent carboxylic acid in *P. falciparum*.

The low antimalarial activity displayed by aminoester **1** (IC_{50} value is 12.6 μM) is in the same range as the IC_{50} values (between 10.8 and 24.1 μM) found for three different ester derivatives of **M$_5$**, previously synthesized from methyl, pivaloyloxymethyl, and *n*-propyloxymethyl alcanols.[8] This suggests that the three esters as well as ester **1** are adsorbed to membranes and other macromolecular constituents in the host milieu and do not penetrate into infected red blood cells. Such a behavior has recently been observed with ester prodrugs of ampicillin (pivaloyloxymethyl, phthalimidomethyl) that were analyzed for membrane-binding properties and membrane penetration.[23] These weak bases were shown to remain located at the cell surface without entering the cell.

The difference in the antiplasmodial activity between aminoesters **1** and **2** may be at least partially attributed to the higher ability of **2** to cross the membranes of infected cells due to the presence of the lipophilic ferrocenyl moiety; the log $P_{octanol/water}$ value for ferrocene was estimated to be 3.28. Indeed, as previously reported for ferroquine,[24] introduction of the metallocenic moiety modifies the physicochemical properties of the 4-aminoquinoline and leads to a higher lipophilicity value, lower flexibility of the side chain, and lower ionization constant (pK_a) of the amine groups, resulting in improved antimalarial effects. In our work, the organometallic alcohol 2-(*N,N*-dimethylaminomethyl)ferrocenylmethanol from ester **2** showed also an antimalarial activity per se, in the same range as that of the carboxylic acid counterpart **M$_5$** (IC_{50} values ca. 3.5 μM). The combination of the carboxylic acid **M$_5$** and the ferrocenyl alcohol resulted in double-drug **2** displaying a higher antimalarial activity than both starting materials, probably through hydrolysis of the ester bond in the parasite. This effect seems to be specifically pronounced in infected red blood cells since cytotoxicity against hMRC-5 cells was observed neither for ester **2** nor for the parent metallocenic alcohol and the carboxylic acids **M$_3$**−**M$_5$**.

The antimalarial action of carboxamides **3**−**5** and the protected tetrazoles **6**−**8** deserves to be discussed with cautious considerations. Although hydrolysis of amide bonds under physiological conditions is less favored than hydrolysis of ester bonds, numerous nonpeptidic amides have been shown to act as prodrugs of carboxylic acids (see ref 25 for a literature review). As a rule they are cleaved in vivo by peptidases. Different members of the protease families involved in hemoglobin degradation could be candidates for the proteolysis of the amide bond in *P. falciparum* to release the GR inhibitor **M$_5$**. Also, nonenzymic hydrolysis of secondary amides to carboxylic acids is well documented: Boc groups[26] and nitroso groups[27,28] change the character of secondary amide bonds to that of imide bonds. In particular, nitrosoamides decompose into carboxylic acids under mild conditions and with high yield. In *Plasmodium*, the formation of dinitrogen trioxide (N_2O_3)—known as a powerful nitrosating agent in vivo[29]—can result from a reaction between nitrogen dioxide (NO_2) and nitric oxide (NO). The steady state levels of nitric oxide and NO_2 are high enough to envision the formation of N_2O_3 in the food vacuole of *P. falciparum* under oxidative stress (Dr. R. Radi, personal communication). Nitrosation reactions were also proposed in acidic compartments due to reactions with nitrous acid (HNO_2). Hence, a preceding nitrosation reaction might promote hydrolysis of carboxamides in the acidic compartments of *Plasmodium* parasites that are exposed to elevated fluxes of reactive nitrogen species and contribute to the release of the parent carboxylic acid.

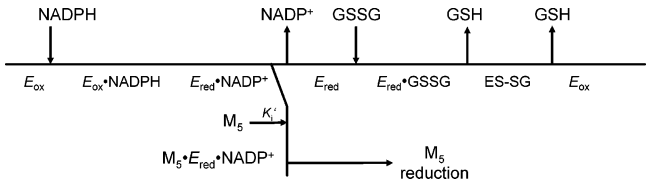

Figure 2. Cleland diagram for dead-end inhibition of *P. falciparum* glutathione reductase by **M$_5$**. Each subunit of the homodimeric flavoenzyme GR contains a redox active disulfide and a flavin cofactor that are in redox contact. This ground state of the enzyme is referred to as E_{ox}. Physiologically, E_{ox} is reduced by NADPH via the flavin, which results in the two-electron-reduced enzyme E_{red} with bound $NADP^+$. When NADPH is in excess, this is followed by an exchange of $NADP^+$ for NADPH. E_{red}, which is characterized by an active site dithiol, then reacts with the second substrate, glutathione disulfide (GSSG), yielding two molecules of reduced glutathione (GSH). During the reductive half-reaction, **M$_5$** is supposed to bind to one of the binary complexes, leading to the formation of the ternary complex, **M$_5$**·E_{red}·$NADP^+$, which is inactive with respect to GSSG reduction, but active in **M$_5$** reduction.

In the case of the three cyanoethyl-protected tetrazoles **6**−**8** we speculate that the cyanoethyl group initially confers sufficient lipophilicity to the molecules for crossing the membranes; subsequently it is removed by base-catalyzed β-H elimination to liberate the tetrazole moiety in the parasites. This is in agreement with the low IC_{50} values evaluated for **6**−**8** in antimalarial assays. Despite the acidic milieu of the food vacuole—the pH being between 5.0 and 5.5—base catalysis is possible, e.g. by the action of accessible histidine residues of parasite protein active sites. It is worth mentioning that different prodrugs of tetrazoles were shown to be a relevant approach to enhance the oral bioavailability of tetrazoles.[9,30]

Uncompetitive Inhibition. M$_5$ inhibits GR through an uncompetitive type with respect to GSSG. Uncompetitive inhibition is often encountered with multisubstrate enzymes, involving the formation of ternary complexes that cannot contribute to the reaction.[31] The pattern of inhibition shows that inhibition by **M$_5$** is reversible. **M$_5$** follows uncompetitive kinetics with respect to both NADPH and GSSG. Since uncompetitive inhibition indicates that the inhibitor is binding after the varied substrate, **M$_5$** must be binding to one of the binary complexes, e.g. to E_{ox}·NADPH or E_{red}·$NADP^+$ (Figure 2).[32] This is consistent with the previous observation that in the course of the reductive half-reaction

$FADH^-$ reoxidation by the catalytic disulfide is the rate-limiting step in catalysis.[33] The potent uncompetitive dead-end inhibition of GR suggests that **M5** might be structurally similar to a tightly bound intermediate in catalysis. The resulting ternary complex $\mathbf{M_5}\cdot E_{red}\cdot NADP^+$ is inactive with respect to GSSG reduction but still active in **M5** reduction.

Uncompetitive inhibition generally leads to dramatic cellular effects because this inhibition type induces positive feedback interactions between target enzyme and substrate that reinforce the inhibition.[31,34] In the present case, the cellular effects of an uncompetitive inhibitor are probably due to increasing and finally toxic GSSG levels that interfere with the viability of the parasites. Consequently, in the parasite redox metabolism, a high GSSG level is expected to potentiate the inhibition of *P. falciparum* GR by **M5**. Thus, the action of **M5** could affect the antioxidant system at different points: first, by inhibiting the GSH regeneration according to the described uncompetitive GR inhibition; and second, by increasing the level of GSSG to concentrations that are toxic to the parasites, and also by increasing the $[NADP^+]/[NADPH]$ ratio through its redox-cycling activity.

Modeling Studies. By combining the GR inhibition studies with the results of the ab initio quantum calculations, the importance of a strong electron-rich group at the end of the hydrophobic alkyl chain in **M5** is clearly shown. This negative charge might allow the establishment of salt bridge interactions with Arg37 and Arg18 of human GR and *P. falciparum* GR, respectively. In addition, comparison of the molecular volumes strongly supports the structural similarity between **M5** and the tetrazole **T4**. It is noteworthy that the activity of the inhibitors could be defined as the sum of different properties such as their affinity for the binding site and their redox behavior. Subversive substrates (turncoat inhibitors) of GR divert electrons from the physiologically catalyzed reactions. Reduction of such molecules may occur at the active site[35] or at different site(s), as it has been suggested for reversible inhibitors such as nitrofurans[36] and quinones.[37] In the case of the garlic-derived ajoene, the compound reacts with the two-electron-reduced enzymes, leading to a mixed disulfide at Cys58 (in human GR) and to an increased NADPH oxidation activity in the modified enzymes, which results in superoxide anion radical production.[35] This finding fits with those obtained by Cenas and coworkers, who reported that trypanothione reductase alkylated by iodoacetamide at Cys52 maintained considerable quinone reductase activity in the presence of juglone.[36] As GR follows a Ping-Pong reaction mechanism, the uncompetitive inhibition type observed for numerous nitrofurans and quinones,[36] and in particular for the **M5** studied here, may indicate the accumulation of dead-end $NADP^+\cdot GR\cdot$inhibitor complexes.[32] The binding mode of **M5** in GR is not yet known. So far, only one crystal structure of a human GR/naphthoquinone complex has been solved; this structure revealed that menadione binds in the large cavity at the dimer interface, which is distinct from the binding sites for GSSG, FAD, and NADPH.[17] Therefore, it is tempting to speculate that the respective cavity in GR is the binding site of **M5**. This cavity is well defined, but its cell physiological role has not yet been elucidated. The structures of several complexes between GR and uncompetitive or noncompetitive ligands are available.[6,17–21] Binding of these ligands at this cavity across the 2-fold axis causes inhibition of the physiological GSSG reduction. However, among these compounds, only menadione, **M5**, and methylene blue are reduced by *P. falciparum* GR. This observation raises the question of the potential site(s) for **M5** reduction. Ligands can have more than one binding site,[38] as illustrated for menadione, which binds, to a lesser extent, also at the NADPH and disulfide sites in human GR.[17] The electron-transfer mechanisms operating between the flavin and naphthoquinone remain speculative until structural studies will reveal if **M5** is reduced at the NADPH site, the disulfide site, or the cavity at the 2-fold axis of the homodimer. A comparison of human GR and *P. falciparum* GR structures revealed that the respective cavities at the 2-fold axis of both enzymes have comparable volumes but are clearly different in shape. Our studies on molecular volumes yield insight into the accessibility of these cavities by a potential ligand. In both enzymes, the cavity is connected to the two catalytic sites by two short primary channels starting near the disulfide substrate binding sites. In human GR, two secondary channels were identified providing a direct access to the surface of the protein. Several residues in the cavity of GR show marked flexibility; in particular those lining the primary channels could be crucial for large ligands to reach the cavity. With respect to the specificity toward *P. falciparum* GR in contrast to human GR, detailed comparisons indicated that 40% (9/22) of the amino acid residues are conserved between both cavities: hydrophobic (Pro387/Pro374 and Leu455/Leu438), polar and uncharged (Thr486/Thr46, Pro389/Pro376, and Pro485/Pro468), acidic (Asp458/Asp441 and Glu459/Glu442), and basic (Lys48/Lys67 and His387/His374). The preference of human GR and *P. falciparum* GR for negatively charged ligands even if they bind in the cavity may be due to the fact that the cavity at the 2-fold axis is accessible via the positively charged GSSG binding site.

Conclusion. In conclusion, the uncompetitive inhibition of *P. falciparum* GR by the naphthoquinone **M5** explains the potent antimalarial action of the double drugs and other prodrugs based on **M5**. The design and synthesis of more potent and specific naphthoquinones as subversive inhibitors of *P. falciparum* GR is in progress. On the basis of these results, the inhibitor structure will now be modified with a focus on preparing new naphthoquinone moieties that increase their binding affinity for *P. falciparum* GR.

Experimental Section

Abbreviations. DCC, *N*,*N*′-dicyclohexylcarbodiimide; DMAP, 4-dimethylaminopyridine; DBU, 1,8-diazabicyclo[5.4.0]undec-7-ene; EDC, *N*,*N*′-1-ethyl-3-(3′-dimethylaminopropyl)carbodiimide; ESI-MS, electrospray ionization mass spectrometry; G6PDH, glucose-6-phosphate dehydrogenase; GR, glutathione reductase; GSH, reduced glutathione; GSSG, glutathione disulfide; HOBt, 1-hydroxybenzotriazole; HPLC t_R, HPLC retention time; MALDI-TOF MS, matrix-assisted laser desorption/ionization time-of-flight mass spectrometry; MB, methylene blue; MEP, molecular electrostatic potential; MV, molecular volume; NQ, naphthoquinone; TBAF, tetrabutylammonium fluoride; TEA, triethylamine.

Enzymes. Recombinant human and *P. falciparum* glutathione reductases (GR, EC 1.6.4.2) were purified as previously reported.[39,40] One unit of GR activity is defined as the consumption of 1 μmol of NADPH/min ($\epsilon_{340\ nm} = 6.22\ mM^{-1}\ cm^{-1}$) under conditions of substrate saturation. The enzyme stock solutions used for kinetic determinations were >98% pure as judged from silver stained SDS−PAGE and had specific activities of 200 units/mg (human GR) and 120 units/mg (*P. falciparum* GR). All other reagents were of the highest available purity and were purchased from Biomol, Boehringer, and Sigma.

Chemicals. The three starting carboxylic acids 6-[2′-(3′-methyl)-1′,4′-naphthoquinolyl]hexanoic acid **M$_5$**, 5-[2′-(3′-methyl)-1′,4′-naphthoquinolyl]pentanoic acid **M$_4$**, and 4-[2′-(3′-methyl)-1′,4′-naphthoquinolyl]butyric acid **M$_3$** were synthesized according to reported procedures.[41] All other chemicals were purchased from Acros and Aldrich and used without further purification. CH_2Cl_2 was distilled under nitrogen atmosphere from $CaCl_2$. The used petroleum ether had a bp of 40−65 °C.

Chemistry. Melting points were determined on a Büchi melting point apparatus and were not corrected. ^{1}H and ^{13}C NMR spectra were recorded on a Bruker DRX-300 MHz spectrometer, and chemical shifts were expressed in ppm relative to TMS; multiplicity was indicated as s (singlet), d (doublet), t (triplet), and m (multiplet). Mass spectra were recorded on a time-of-flight plasma desorption mass spectrometer (TOF-PDMS) using a californium source; alternatively MALDI-TOF mass spectra (MALDI-TOF MS) were obtained using a Voyager DE-STR time-of-flight instrument (Applied biosystems, Palo Alto, CA) equipped with a nitrogen laser operating at 337 nm. Between 50 and 100 laser shots were accumulated in the reflector mode to obtain a good signal-to-noise ratio. The matrix used was α-cyano-4-hydroxycinnamic acid (αCHCA). Alternately electrospray-ionization mass spectra (ESI-MS) were performed at the Biochemie-Zentrum of Heidelberg University in the department of Dr. J. Lechner. New derivatives were isolated by silica gel chromatography of the crude reaction mixture. The purity (P_{HPLC}) of the isolated compounds was checked by elemental analysis or by two types of high pressure liquid chromatography (HPLC) columns, a Macherey-Nagel C18 Nucleosil column (4 × 300 mm, 5 μm, 100 Å) or a C18 Vydac 218 TP column (4 × 300 mm, 5 μm, 100 Å). Analytical HPLC was performed on a Shimadzu system equipped with a UV detector set at 254 nm. Compounds were dissolved in EtOH and injected through a 50 μL loop. The following solvent systems were used: eluent (A), 0.05% trifluoroacetic acid (TFA) in H_2O; eluent (B), 0.05% TFA, 20% H_2O, 80% CH_3CN. HPLC retention times (HPLC t_R) were obtained at flow rates of 1 mL/min, using the following conditions: 100% eluent A for 5 min, then a gradient run to 100% eluent B over the next 30 min. Elemental analyses were performed at Organisch-Chemisches Institut, Heidelberg University.

General Procedure for the Preparation of the Esters 1 and 2. A mixture of 6-[2′-(3′-methyl)-1′,4′-naphthoquinolyl]-hexanoic acid **M$_5$** (1 mmol), alcohol (24 equiv for MeOH and 1 equiv for other alcohols), and 4-dimethylaminopyridine (0.4 mmol) in dry CH_2Cl_2 (20 mL) was stirred in an ice bath. After addition of DCC (1.1 mmol), the mixture was stirred at room temperature for 24 h and then filtered. The filtrate was washed with 5% aqueous $NaHCO_3$ (2 × 25 mL) and brine (2 × 25 mL), dried with Na_2SO_4, and then submitted to evaporation. The crude residue was then purified by silica gel chromatography to yield the desired aminoester derivatives **1** and **2**, using EtOAc/petroleum ether/TEA (7:2:1) and EtOAc/TEA (9:1), respectively.

6-[2′-(3′-Methyl)-1′,4′-naphthoquinolyl]hexanoic acid 2-dimethylamino-ethyl ester 1: obtained from alcohol *N,N*-dimethylaminoethanol (383 mg, 4.3 mmol) and **M$_5$** (245 mg, 0.086 mmol) as a yellow oil (60 mg, 0.17 mmol, 20% yield). ^{1}H NMR ($CDCl_3$): δ 8.07 (2H, m, NQ), 7.69 (2H, m, NQ), 4.17 (2H, t, J = 5.8 Hz, CH_2), 2.64 (2H, t, J = 7.9 Hz, CH_2), 2.56 (2H, t, J = 5.8 Hz, CH_2), 2.35 (2H, t, J = 7.5 Hz, CH_2), 2.28 (6H, s, $N(CH_3)_2$), 2.19 (3H, s, CH_3), 1.71 (2H, m, CH_2), 1.49 (4H, m, $2CH_2$). MALDI-TOF MS (thap): 359 ($M^{\bullet+}$). HPLC (C_{18} Nucleosil): t_R 23.0 min. HPLC (C_{18} Vydac): t_R 21.0 min.

6-[2′-(3′-Methyl)-1′,4′-naphthoquinolyl]hexanoic acid [2-dimethylaminomethyl)ferrocenyl]methyl ester 2: obtained from alcohol 2-(*N,N*-dimethylaminomethyl)ferrocenylmethanol (148 mg, 0.54 mmol) and **M$_5$** (155 mg, 0.54 mmol) as an orange oil (170 mg, 0.31 mmol, 58% yield). ^{1}H NMR ($CDCl_3$): δ 8.07 (2H, m, NQ), 7.69 (2H, m, NQ), 5.00 (1H, d, J = 12.3 Hz, CH), 4.90 (1H, d, J = 12.3 Hz, CH), 4.33 (1H, m, CH), 4.30 (1H, m, CH), 4.20 (1H, m, CH), 4.10 (5H, s, Cp′), 3.54 (1H, d, J = 13.1 Hz, CH), 3.36 (1H, d, J = 13.1 Hz, CH), 2.62 (2H, t, J = 7.4 Hz, CH_2), 2.29 (2H, t, J = 7.4 Hz, CH_2), 2.22 (6H, s, $N(CH_3)_2$), 2.18 (3H, s, CH_3), 1.67 (2H, m, CH_2), 1.46 (4H, m, $2CH_2$). MALDI-TOF MS (thap): 541 ($M^{\bullet+}$). HPLC (C_{18} Nucleosil): t_R 31.4 min.

5-[2′-(3′-Methyl)-1′,4′-naphthoquinolyl]pentanoic Acid (2-Cyanoethyl) Amide 4. To a stirred solution of 3-aminopropionitrile (582 mg, 8.3 mmol) in DMF (15 mL) was added **M$_4$** (1.51 g, 5.5 mmol) followed by HOBt (748 mg, 5.5 mmol). The mixture was cooled to 0 °C with an ice bath, and EDC (1.11 g, 7.2 mmol) was added. After stirring for 1 h at 0 °C and then for 5 h at ambient temperature, the reaction mixture was diluted in EtOAc (75 mL) and washed successively with 1 M HCl (25 mL), brine (25 mL), 5% $NaHCO_3$ solution (25 mL), and brine again (25 mL). The organic layer was dried over $MgSO_4$ and concentrated under reduced pressure. The crude product was purified by recrystallization using acetone/petroleum ether (1:2) to give **4** as a yellow solid (1.45 g, 4.5 mmol, 82%): mp 138−139 °C. ^{1}H NMR ($CDCl_3$): δ 8.03 (2H, m, NQ), 7.66 (2H, m, NQ), 6.28 (1H, m, NH), 3.49 (2H, q, J = 6.2 Hz, CH_2), 2.63 (4H, t, J = 6.2 Hz, $2CH_2$), 2.27 (2H, t, J = 7.4 Hz, CH_2), 2.16 (3H, s, CH_3), 1.75 (2H, m, CH_2), 1.50 (2H, m, CH_2). ^{13}C NMR ($CDCl_3$): δ 185.14, 184.82, 173.30, 146.63, 143.57, 133.40, 133.36, 132.12, 132.08, 126.22, 118.18, 35.81, 35.68, 27.82, 26.40, 25.55, 18.42, 12.65. ESI-MS: 324.97 ($M^{\bullet+}$). Anal. ($C_{19}H_{20}N_2O_3 \cdot 0.25H_2O$): calcd C 69.39, H 6.28, N 8.52; found C, H, N.

4-[2′-(3′-Methyl)-1′,4′-naphthoquinolyl]butyric acid (2-cyanoethyl)amide 3: obtained from **M$_3$**, according to the preparation of amide **4**. ^{1}H NMR ($CDCl_3$): δ 8.07 (2H, m, NQ), 7.71 (2H, m, NQ), 6.46 (1H, m, NH), 3.54 (2H, q, J = 6.2 Hz, CH_2), 2.67 (4H, 2t, J = 6.2 and 7.1 Hz, $2CH_2$), 2.33 (2H, t, J = 7.1 Hz, CH_2), 2.22 (3H, s, CH_3), 1.82 (2H, m, CH_2). ESI-MS: 310.11 ($M^{\bullet+}$). HPLC (C_{18} Nucleosil): 22.5 min. HPLC (C_{18} Vydac): 20.1 min.

6-[2′-(3′-Methyl)-1′,4′-naphthoquinolyl]hexanoic acid (2-cyanoethyl) amide 5: obtained from **M$_5$** (588 mg, 2.1 mmol), according to the preparation of amide **4**, as a yellow solid (618 mg, 1.8 mmol, 87%). Mp: 73−74 °C. ^{1}H NMR ($CDCl_3$): δ 8.08 (2H, m, NQ), 7.70 (2H, m, NQ), 6.31 (1H, m, NH), 3.50 (2H, q, J = 6.2 Hz, CH_2), 2.63 (4H, t, J = 6.2 Hz, $2CH_2$), 2.24 (2H, t, J = 7.5 Hz, CH_2), 2.18 (3H, s, CH_3), 1.71 (2H, m, CH_2), 1.48 (4H, m, $2CH_2$). MALDI-TOF MS (thap): 338 ($M^{\bullet+}$). HPLC (C_{18} Nucleosil): 25.4 min. HPLC (C_{18} Vydac): 22.6 min.

3-{5-[4-[2′-(3′-Methyl)-1′,4′-naphthoquinolyl]butyl]tetrazol-1-yl}propionitrile 7. Triflic anhydride (2.1 mL, 12.4 mmol) was added to a stirred suspension of **4** (1.0 g, 3.1 mmol) and sodium azide (605 mg, 9.3 mmol) in CH_3CN (35 mL) under nitrogen atmosphere. The mixture rapidly resulted in a homogeneous solution. After 20 h, the mixture was poured into 5% $NaHCO_3$ solution (25 mL) and extracted with EtOAc (2 × 25 mL). The combined organic phases were washed with brine (2 × 25 mL), then dried over $MgSO_4$, and concentrated under reduced pressure. The crude oil was recrystallized using acetone/petroleum ether (2:1) to give **7** as a yellow solid (810 mg, 2.3 mmol, 75%): mp 123−124 °C. ^{1}H NMR ($CDCl_3$): δ 8.09 (2H, m, NQ), 7.73 (2H, m, NQ), 4.66 (2H, t, J = 6.7 Hz, CH_2), 3.10 (2H, t, J = 6.7 Hz, CH_2), 2.98 (2H, t, J = 7.6 Hz, CH_2), 2.67 (2H, t, J = 7.7 Hz, CH_2), 2.17 (3H, s, CH_3), 1.95 (2H, m, CH_2), 1.61 (2H, m, CH_2). ^{13}C NMR ($CDCl_3$): δ 184.84, 184.68, 154.97, 145.99, 143.68, 133.30, 133.23, 131.89, 131.77, 126.08, 126.01, 115.61, 42.19, 27.54, 26.77, 25.86, 22.40, 18.59,

12.52. ESI-MS: 349.86 ($M^{\bullet+}$). Anal. ($C_{19}H_{19}N_5O_2$, 0.5 H_2O) calcd C 63.67, H 5.62, N 19.54; found C, H, N.

3-{5-[5-[2′-(3′-Methyl)-1′,4′-naphthoquinolyl]pentyl]tetrazol-1-yl}propionitrile 8: obtained from **5** (155 mg, 0.4 mmol), according to the preparation of propionitrile **7**, as a yellow oil (102 mg, 0.3 mmol, 70%). ^{1}H NMR ($CDCl_3$): δ 8.06 (2H, m, NQ), 7.70 (2H, m, NQ), 4.65 (2H, t, J = 6.7 Hz, CH_2), 3.15 (2H, t, J = 6.7 Hz, CH_2), 2.96 (2H, t, J = 7.6 Hz, CH_2), 2.63 (2H, m, CH_2), 2.16 (3H, s, CH_3), 1.94 (2H, m, CH_2), 1.55 (4H, m, $2CH_2$). MALDI-TOF MS: (thap) 363 ($M^{\bullet+}$). HPLC (C_{18} Nucleosil): 26.1 min. HPLC (C_{18} Vydac): 24.0 min.

3-{5-[3-[2′-(3′-Methyl)-1′,4′-naphthoquinolyl]propyl]tetrazol-1-yl}propionitrile 6: obtained from **3**, according to the preparation of propionitrile **7**. ^{1}H NMR ($CDCl_3$): δ 8.05 (2H, m, NQ), 7.69 (2H, m, NQ), 4.65 (2H, t, J = 6.7 Hz, CH_2), 3.15 (2H, t, J = 6.7 Hz, CH_2), 2.96 (2H, t, J = 7.6 Hz, CH_2), 2.63 (2H, t, J = 7.6 Hz, CH_2), 2.17 (3H, s, CH_3), 1.91 (2H, m, CH_2) 1.61. ^{13}C NMR ($CDCl_3$): δ 185.58, 185.28, 155.79, 147.14, 143.92, 134.93, 133.86, 132.49, 126.65, 116.32, 42.79, 29.30, 28.60, 26.95, 26.87, 23.09, 19.23, 13.09. HPLC (C_{18} Nucleosil): 26.1 min. HPLC (C_{18} Vydac): 23.9 min.

2-Methyl-3-[4-(1*H*-tetrazol-5-yl)butyl]-[1,4]naphthoquinone T_4. To a stirred solution of **7** (500 mg, 1.43 mmol) in THF (10 mL) was added a solution of $LiOH·H_2O$ (72 mg, 1.72 mmol, 1.2 equiv) in methanol (3 mL). After stirring at room temperature for 2 h, the mixture was diluted with water (100 mL) and washed with EtOAc (2 × 25 mL). The aqueous layer was acidified with 1 M HCl and extracted with EtOAc (3 × 25 mL), dried over $MgSO_4$, and concentrated under reduced pressure. The crude residue was purified by silica gel chromatography using EtOAc/MeOH (9:1) to yield the desired tetrazole $\mathbf{T_4}$ (380 mg, 1.28 mmol, 90%). ^{1}H NMR (DMSO): δ 7.85−8.15 (4H, m, NQ), 2.8−3.1 (4H, m, CH_2), 2.13 (3H, s, CH_3), 1.4−1.95 (4H, m, CH_2). MALDI-TOF MS (thap): 296.13 ($M^{\bullet+}$).

2-Methyl-3-[5-(1*H*-tetrazol-5-yl)pentyl]-[1,4]naphthoquinone T_5: obtained from **8** (142 mg, 0.39 mmol), in analogy to the preparation of tetrazole $\mathbf{T_4}$, as an orange powder (80 mg, 0.26 mmol, 67% yield). ^{1}H NMR ($CDCl_3$): δ 8.05 (2H, m, NQ), 7.72 (2H, m, NQ), 3.06 (2H, t, J = 7.5 Hz, CH_2), 2.62 (2H, t, J = 7.3 Hz, CH_2), 2.17 (3H, s, CH_3), 1.93 (2H, m, CH_2), 1.52 (4H, m, $2CH_2$). MALDI-TOF MS (thap): 310.35 ($M^{\bullet+}$).

GR Inhibition Studies. All kinetic studies were carried out at 25 °C in a volume of 1 mL. The assay mixtures contained 100 mM potassium phosphate buffer pH 7.0, 200 mM KCl, 100 μM NADPH, and 1 mM GSSG. Inhibitor stock solutions were prepared in 100% DMSO. One % final DMSO concentration was kept constant in the assay cuvette. The reaction was started with the addition of the enzyme (8 milliunits or 1.2 pmol of FAD-containing subunit in 5 μL aliquot), and initial rates were determined from NADPH oxidation measured at 340 nm.

(a) IC_{50} Determinations. The standard assay mixture contained 100 μM NADPH and 1 mM GSSG. IC_{50} values were evaluated in duplicate in the presence of 10 inhibitor concentrations ranging from 0 to 200 μM. The reaction was started by adding enzyme (8 milliunits), and NADPH oxidation was monitored at 340 nm.

(b) Evaluation of Inhibition Type and K_i. Type of inhibition and inhibition constants for $\mathbf{M_5}$ were determined in duplicate experiments. *P. falciparum* GR activity was measured at different concentrations of $\mathbf{M_5}$ (0, 2, 5, and 10 μM), either in the presence of varying concentrations of NADPH (8−100 μM) at a constant GSSG concentration of 1 mM or in the presence of varying concentrations of GSSG (18−900 μM) at a constant NADPH concentration of 100 μM. K_m and V_{max} values were determined by fitting data to the Michaelis−Menten equation using nonlinear regression analysis.[32] Inhibition of GSSG reduction by $\mathbf{M_5}$ was measured as a function of substrate concentration, and the data were fitted by using nonlinear regression analysis software (Kaleidagraph) to the equation for uncompetitive inhibition:

$$V = \frac{V_{max}[S]}{K_m + [S]\{1 + ([I]/K_i)\}}$$

(c) Kinetics in the Presence of NADPH-Regenerating System or Exogenous $NADP^+$. In experiments where it was desirable to have no significant quantities of $NADP^+$ present, an NADPH-regenerating system consisting of glucose-6-phosphate and G6PDH was applied. To a mixture of 20 milliunits of G6PDH, 1 mM GSSG, 1 mM glucose-6-phosphate, and DMSO or inhibitor solution, 100 μM NADPH was added in the cuvette. The final concentration of DMSO was kept constant to 1.6% in the assay cuvette. Disulfide reduction was then followed spectrophotometrically at 340 nm. In experiments where the influence of exogenous $NADP^+$ was studied, the IC_{50} values were evaluated in the presence or absence of 200 μM $NADP^+$ in the GR assay using 1 mM GSSG and 100 μM NADPH.

***P. falciparum* GR-Catalyzed Naphthoquinone Reductase Activity.** The ability of *P. falciparum* GR to reduce the naphthoquinone was assayed by monitoring the oxidation of NADPH at 340 nm ($\epsilon_{340\ nm}$ = 6.22 mM^{-1} cm^{-1}). The assay mixtures, in a total volume of 1 mL, contained 100 mM phosphate buffer pH 7.0, 200 mM KCl, 100 μM NADPH, and 3.9 units of *P. falciparum* GR. The naphthoquinone was dissolved in DMSO, and the NADPH-oxidation activity was measured at 10 different inhibitor concentrations (10−400 μM) in the presence of 1% DMSO. For the determination of K_m and V_{max} values, the steady-state rates were graphically fitted by using nonlinear regression analysis software (Kaleidagraph) to the Michaelis−Menten equation,[32] and the turnover number k_{cat} and the catalytic efficiency k_{cat}/K_m were calculated. The initial rate for intrinsic NADPH oxidation activity of *P. falciparum* GR was not subtracted from the rates measured in the presence of the naphthoquinone when it proved negligible in comparison to GR-catalyzed naphthoquinone reductase activity.

Ab Initio Quantum Chemistry Energy Calculations. All ab initio energy calculations were carried out using the Gaussian 98 suite of programs.[42] The deprotonated forms of the compounds $\mathbf{M_3}$−$\mathbf{M_5}$ and $\mathbf{T_3}$−$\mathbf{T_5}$ were used in this study because it is the anionic form which is assumed to interact with GR. The structures were built using the CORINA program.[43] The geometries of the compounds were optimized at the Hartree−Fock (HF) level using the polarized split-valence 6-31G** basis set.[44,45] All stationary points were shown to be minima by frequency calculations at the same level. The molecular electronic properties of the studied compounds such as molecular electrostatic potentials and molecular orbital energies were calculated at the HF/6-31G** level. The molecular electrostatic potential map (MEP) isoenergy contours were superimposed onto the total electron density surface (0.002 e/au^3). Charge distributions were calculated at HF/6-31G** level using the Mulliken population analysis. MP2 levels were computed considering the sum of the Hartree−Fock (HF) energies and electron correlation contributions, $\Delta E_{MP2} = \Delta E_{HF} + \Delta E_{Cor}$, using the 6-31G** basis set.[46]

Acknowledgment. Irene König, Heidelberg University, and Gérard Montagne, Lille University, are gratefully acknowledged for *P. falciparum* glutathione reductase assays and NMR spectra, respectively. Initial studies on menadione as an uncompetitive inhibitor of human GR were conducted by Dr. Axel Nordhoff, Heidelberg. Dr. Philippe Grellier and Dr. Louis Maes are acknowledged for antimalarial assays of the two esters **1** and **2** and for cytotoxicity assays against the human cell line hMRC-5. Our work is supported by the CNRS-DFG program (E.D.-C. and R.H.S.), the Deutsche Forschungsgemeinschaft (SFB 544) (R.H.S.), and the VIHPAL Program of the Ministère de l'Education Nationale, de la Recherche et de la Technologie (fellowship

attributed to C.B.). C.B. also acknowledges support from the Belgian National Fund for Scientific Research (FNRS).

References

(1) Schirmer, R. H.; Müller, J. G.; Krauth-Siegel, R. L. Disulfide reductase inhibitors as chemotherapeutic agents: the design of drugs for trypanosomiasis and malaria. *Angew. Chem., Int. Ed. Engl.* **1995**, *34*, 141−154.

(2) Krauth-Siegel, R. L.; Bauer, H.; Schirmer, R. H. Dithiol proteins as guardians of the intracellular redox milieu in parasites. Old and new drug targets in trypanosomes and malaria-causing plasmodia. *Angew. Chem., Int. Ed. Engl.*, in press.

(3) Ginsburg, H.; Famin, O.; Zhang, J.; Krugliak, M. Inhibition of glutathione-dependent degradation of heme by chloroquine and amodiaquine as a possible basis for their antimalarial mode of action. *Biochem. Pharmacol.* **1998**, *56*, 1305−1313.

(4) Meierjohann, S.; Walter, R. D.; Müller, S. Regulation of intracellular glutathione levels in erythrocytes infected with chloroquine-sensitive and chloroquine-resistant *Plasmodium falciparum*. *Biochem. J.* **2002**, *368*, 761−768.

(5) Deharo, E.; Barkan, D.; Krugliak, M.; Golenser, J.; Ginsburg H. Potentiation of the antimalarial action of chloroquine in rodent malaria by drugs known to reduce cellular glutathione levels. *Biochem. Pharmacol.* **2003**, *66*, 809−817.

(6) Sarma, G. N.; Savvides, S. N.; Becker, K.; Schirmer, M.; Schirmer, R. H.; Karplus, P. A. Glutathione reductase of the malarial parasite *Plasmodium falciparum*: crystal structure and inhibitor development. *J. Mol. Biol.* **2003**, *328*, 893−907.

(7) Karplus, P. A.; Pai, E. F.; Schulz, G. E. A crystallographic study of the glutathione binding site of glutathione reductase at 0.3-nm resolution. *Eur. J. Biochem.* **1989**, *178*, 693−703.

(8) Davioud-Charvet, E.; Delarue, S.; Biot, C.; Schwöbel, B.; Böhme, C. C.; Müssigbrodt, A.; Maes, L.; Sergheraert, C.; Grellier, P.; Schirmer, R. H.; Becker, K. A prodrug form of a *Plasmodium falciparum* glutathione reductase inhibitor conjugated with a 4-anilinoquinoline. *J. Med. Chem.* **2001**, *44*, 4268−4276.

(9) Herr, R. J. 5-Substituted-1*H*-tetrazoles as carboxylic acid isosteres: medicinal chemistry and synthetic methods. *Bioorg. Med. Chem.* **2002**, *10*, 3379−3393.

(10) Koguro, K.; Oga, T.; Mitsui, S.; Orita, R. Novel synthesis of 5-substituted tetrazoles from nitriles. *Synthesis* **1998**, 910−914.

(11) De Lombaert, S.; Blanchard, L.; Stamford, L. B.; Tan, J.; Wallace, E. M.; Satoh, Y., Fitt; J., Hoyer, D.; Simonsbergen, D.; Moliterni, J.; Marcopoulos, N.; Savage, P.; Chou, M.; Trapani, A. J.; Jeng, A. Y. Potent and selective non-peptidic inhibitors of endothelin-converting enzyme-1 with sustained duration of action. *J. Med. Chem.* **2000**, *43*, 488−504.

(12) Biot, C.; Dessolin, J.; Grellier, P.; Davioud-Charvet, E. Double-drug development against antioxidant enzymes from *Plasmodium falciparum*. *Redox Rep.* **2003**, *8*, 280−283.

(13) Cornish-Bowden, A. A simple graphical method for determining the inhibition constants of mixed, uncompetitive and non-competitive inhibitors. *Biochem. J.* **1974**, *137*, 143−144.

(14) Nordhoff, A. Zur planvollen Entwicklung von Inhibitoren der obligat dimeren Glutathionreduktasen des Menschen und der Maus. Evaluierung potentieller Chemotherapeutika und Ansätze zur Hemmung der Dimerisierung. Ph.D. Thesis, Heidelberg University, 1995.

(15) Blumenstiel, K.; Schöneck, R.; Yardley, V.; Croft, S. L.; Krauth-Siegel, R. L. Nitrofuran drugs as common subversive substrates of Trypanosoma cruzi lipoamide dehydrogenase and trypanothione reductase. *Biochem. Pharmacol.* **1999**, *58*, 1791−1799.

(16) Karplus, P. A.; Schulz, G. E. Refined structure of glutathione reductase at 1.54 Å resolution. *J. Mol. Biol.* **1987**, *195*, 701−729.

(17) Karplus, P. A.; Pai, E. F.; Schulz, G. E. A crystallographic study of the glutathione binding site of glutathione reductase at 0.3-nm resolution. *Eur. J. Biochem.* **1989**, *178*, 693−703.

(18) Savvides, S.; Karplus, P. A. Kinetics and crystallographic analysis of human glutathione reductase in complex with a xanthene inhibitor. *J. Biol. Chem.* **1996**, *271*, 8101−8107.

(19) Schönleben-Janas, A.; Kirsch, P.; Mittl, P. R. E.; Schirmer, R. H.; Krauth-Siegel, L. Inhibition of human glutathione reductase by 10-arylisoalloxazines: crystallographic, kinetic, and electrochemical studies. *J. Med. Chem.* **1996**, *39*, 1549−1554.

(20) Krauth-Siegel, R. L.; Arscott, L. D.; Schönleben-Janas, A.; Schirmer, R. H.; Williams, C. H. Role of active site tyrosine residues in catalysis by human glutathione reductase. *Biochemistry* **1998**, *37*, 13968−13977.

(21) Zappe, H. Die Bindungsstellen hämolyseinduzierender Pharmaka an der Glutathionreduktase aus menschlichen Erythrocyten. M.D. thesis, Heidelberg University, 1980.

(22) Politzer, P.; Truhlar, D. G. *Chemical Applications of Molecular and Electrostatic Potentials*; Politzer, P., Truhlar, D. G., Eds.; Plenum Press: New York, 1981.

(23) Chanteux, H.; Paternotte, I.; Mingeot-Leclercq, M. P.; Brasseur, R.; Sonveaux, E.; Tulkens, P. M. Cell handling, membrane-binding properties, and membrane-penetration modeling approaches of pivampicillin and phthalimidomethylampicillin, two basic esters of ampicillin, in comparison with chloroquine and azithromycin. *Pharm. Res.* **2003**, *20*, 624−631.

(24) Biot, C. Ferroquine: a new weapon in the fight against malaria. *Curr. Med. Chem.* **2004**, *3*, 135−148.

(25) Wermuth, C. G. Designing prodrugs and bioprecursors. In *The practice of medicinal chemistry,* 2nd ed.; Wermuth, C. G., Ed.; Academic Press: London, 2003; pp 561−585.

(26) Beria, I.; Nesi, M. Syntheses of brostallicin starting from distamycin A. *Tetrahedron Lett.* **2002**, *43*, 7323−7327.

(27) Evans, D. A.; Barrow, J. C.; Watson, P. S.; Ratz, A. M.; Dinsmore, C. J.; Evrard, D. A.; DeVries, K. M.; Ellman, J. A.; Rychnovsky, S. D.; Lacour, J. Approaches to the synthesis of the vancomycin antibiotics. Synthesis of orienticin C (bis-dechlorovancomycin) aglycon. *J. Am. Chem. Soc.* **1997**, *119*, 3419−3420.

(28) Evans, D. A.; Katz, J. L.; Peterson, G. S.; Hintermann, T. Total synthesis of teicoplanin aglycon. *J. Am. Chem. Soc.* **2001**, *123*, 12411−12413.

(29) Kirsch, M.; Fuchs, A.; de Groot, H. Regiospecific nitrosation of N-terminal-blocked tryptophan derivatives by N_2O_3 at physiological pH. *J. Biol. Chem.* **2003**, *278*, 11931−11936.

(30) Heerding, J. M.; Lampe, J. W.; Darges, J. W.; Stamper, M. L. Protein kinase C inhibitory activities of balanol analogs bearing carboxylic acid replacements. *Bioorg. Med. Chem. Lett.* **1995**, *5*, 1839−1842.

(31) Cornish-Bowden, A. Why is uncompetitive inhibition so rare? A possible explanation, with implications for the design of drugs and pesticides. *FEBS Lett.* **1986**, *203*, 3−6.

(32) Segel, I. H. (1975) In *Enzyme Kinetics. Behavior and analysis of rapid equilibrium and steady-state enzyme systems*; John Wiley and Sons: New York, 1975.

(33) Böhme, C. C.; Arscott, L. D.; Becker, K.; Schirmer, R. H.; Williams, C. H., Jr. Kinetic characterization of glutathione reductase from the malarial parasite *Plasmodium falciparum*. Comparison with the human enzyme. *J. Biol. Chem.* **2000**, *275*, 37317−37323.

(34) Eisenthal, R.; Cornish-Bowden, A. Prospects for antiparasitic drugs. The case of *Trypanosoma brucei*, the causative agent of African sleeping sickness. *J. Biol. Chem.* **1998**, *273*, 5500−5505.

(35) Gallwitz, H.; Bonse, S.; Martinez-Cruz, A.; Schlichting, I.; Schumacher, K.; Krauth-Siegel, R. L. Ajoene is an inhibitor and subversive substrate of human glutathione reductase and *Trypanosoma cruzi* trypanothione reductase: crystallographic, kinetic, and spectroscopic studies. *J. Med. Chem.* **1999**, *42*, 364−372.

(36) Cenas, N.; Bironaite, D.; Dickancaite, E.; Anusevicius, Z.; Sarlauska, J.; Blanchard, J. S. Chinifur, a selective inhibitor and "subversive substrate" for *Trypanosoma congolense* trypanothione reductase. *Biochem. Biophys. Res. Commun.* **1994**, *204*, 224−229.

(37) Cenas, N. K.; Arscott, D.; Williams, C. H., Jr.; Blanchard, J. S. Mechanism of reduction of quinones by *Trypanosoma congolense* trypanothione reductase. *Biochemistry* **1994**, *33*, 2509−2515.

(38) Bonse, S.; Richards, J. M.; Ross, S. A.; Lowe, G.; Krauth-Siegel, R. L. (2,2′:6′,2″-terpyridine)platinum(II) complexes are irreversible inhibitors of *Trypanosoma cruzi* trypanothione reductase but not of human glutathione reductase. *J. Med. Chem.* **2000**, *43*, 4812−4821.

(39) Nordhoff, A.; Bücheler, U. S.; Werner, D.; Schirmer, R. H.Folding of the four domains and dimerization are impaired by the Gly446→Glu exchange in human glutathione reductase. Implications for the design of antiparasitic drugs. *Biochemistry* **1993**, *32*, 4060−4066.

(40) Färber, P. M.; Arscott, L. D.; Williams, C. H., Jr.; Becker, K.; Schirmer, R. H. Recombinant *Plasmodium falciparum* glutathione reductase is inhibited by the antimalarial dye methylene blue. *FEBS Lett.* **1998**, *422*, 311−314.

(41) Salmon-Chemin, L.; Buisine, E.; Yardley, V.; Kohler, S.; Debreu, M. A.; Landry, V.; Sergheraert, C.; Croft, S. L.; Krauth-Siegel, L. R.; Davioud-Charvet, E. 2- and 3-Substituted-1,4-naphthoquinone derivatives as subversive substrates of trypanothione reductase and lipoamide dehydrogenase from *Trypanosoma cruzi*: synthesis and correlation between redox cycling activities and in vitro cytotoxicity. *J. Med. Chem.* **2001**, *44*, 548−565.

(42) Frisch, M. J.; Trucks, G. W.; Schlegel, H. B.; Scuseria, G. E.; Robb, M. A.; Cheeseman, J. R.; Zakrzewski, V. G.; Montgomery, J. A.; Stratmann, R. E., Jr.; Burant, J. C.; Dapprich, S.; Millam, J. M.; Daniels, A. D.; Kudin, K. N.; Strain, M. C.; Farkas, O.; Tomasi, J.; Barone, V.; Cossi, M.; Cammi, R.; Mennucci, B.; Pomelli, C.; Adamo, C.; Clifford, S.; Ochterski, J.; Petersson, G. A.; Ayala, P. Y.; Cui, Q.; Morokuma, K.; Malick, D. K.; Rabuck, A. D.; Raghavachari, K.; Foresman, J. B.; Cioslowski, J.; Ortiz, J. V.; Baboul, A. G.; Stefanov, B. B.; Liu, G.; Liashenko, A.;

Piskorz, P.; Komaromi, I.; Gomperts, R.; Martin, R. L.; Fox, D. J.; Keith, T.; Al-Laham, M. A.; Peng, C. Y.; Nanayakkara, A.; Gonzalez, C.; Challacombe, M.; Gill, P. M. W.; Replogle, S.; Pople, J. A. *Gaussian 98*, revision A.7; Gaussian, Inc.: Pittsburgh, PA, 1988.

(43) http://www2.chemie.uni-erlangen.de/software/corina/.

(44) Ditchfield, R.; Hehre, W. J.; Pople, J. A. Self-consistent molecular-orbital methods. IX. An extended Gaussian-type basis for molecular-orbital studies of organic molecules. *J. Chem. Phys.* **1971**, *54*, 724−728.

(45) Harinharan, P. C.; Pople, J. A. The influence of polarization functions on molecular orbital hydrogenation energies. *Theor. Chim. Acta* **1973**, *28*, 213−222.

(46) Møller, C.; Plesset, M. S. Note on the approximation treatment for many-electron systems. *Phys. Rev.* **1934**, *46*, 618−622.

(47) MOLEKEL 4.0, P. Flükiger, H. P. Lüthi, S. Portmann, J. Weber, Swiss Center for Scientific Computing, Manno (Switzerland), 2000. See http://www.cscs.ch/molekel/.

JM0497545